Copy No. 329

RM No. L6L26

CONFIDENTIAL

RESEARCH MEMORANDUM

FREE-FALL MEASUREMENTS AT TRANSONIC VELOCITIES OF THE DRAG OF A WING-BODY CONFIGURATION CONSISTING OF A 45° SWEPT-BACK WING MOUNTED FORWARD OF THE MAXIMUM DIAMETER ON A BODY OF FINENESS RATIO 12

By

Charles W. Mathews and Jim Rogers Thompson

Langley Memorial Aeronautical Laboratory
Langley Field, Va.

NATIONAL ADVISORY COMMITTEE FOR AERONAUTICS

WASHINGTON

April 2, 1947

CONFIDENTIAL

NATIONAL ADVISORY COMMITTEE FOR AERONAUTICS

RESEARCH MEMORANDUM

FREE-FALL MEASUREMENTS AT TRANSONIC VELOCITIES OF THE DRAG OF A WING-BODY CONFIGURATION CONSISTING OF A 45° SWEPT-BACK WING MOUNTED FORWARD OF THE MAXIMUM DIAMETER ON A BODY OF FINENESS RATIO 12

By Charles W. Mathews and Jim Rogers Thompson

SUMMARY

The National Advisory Committee for Aeronautics is measuring drag of a series of complete airplane-like configurations and their various components at transonic velocities by the free-fall method. This report covers a test of one configuration of this series. The configuration was composed of a 45° swept-back wing of aspect ratio 4.1 mounted forward of the maximum diameter of a 10-inch-diameter body of fineness ratio 12 equipped with stabilizing tail fins. The wing had a 70-inch span and incorporated an NACA 65-009 airfoil section of 12-inch chord perpendicular to the leading edge. The body-tail fin combination was externally identical with a combination tested previously by this method.

The results are presented as curves showing the variation of drag coefficient with Mach number for the complete configuration and for each component. These results show that the drag per unit frontal area of the complete configuration rose abruptly from 0.06 of atmospheric pressure at a Mach number of 0.89 to 0.167 of atmospheric pressure at a Mach number of 1.02 and then increased at a slower rate to 0.233 at a Mach number of 1.19. At Mach numbers in excess of unity the wing and body shared about equal portions of the total drag (about 42 percent each). The remainder of the total drag (16 percent) was contributed by the stabilizing tail surfaces. Slightly below the velocity of sound the wing drag rose abruptly and at a Mach number of 1 was double the value estimated from previous tests of comparable 45° swept-back airfoils mounted on cylindrical bodies, as no abrupt increase in drag occurred for these previously tested airfoils. After the abrupt rise the wing drag gradually approached values estimated from the previous tests. The body drags measured in this test were higher than those measured in previous tests of an identical body without wings by about 15 percent at a Mach number of 1.05 and 8 percent at 1.15.

INTRODUCTION

A series of tests is being conducted at the Langley Memorial Aeronautical Laboratory of the NACA in which drag measurements are made in the transonic velocity range on test shapes by the free-fall method. The object of these tests is to determine bodies, airfoils, and wing-body combinations which have a minimum of drag at transonic velocities. Results of previous tests of bodies and airfoils by this method (references 1 to 3) have indicated that appreciable reductions in drag at transonic velocities could be obtained by increasing the fineness ratio of bodies of revolution and by using swept-back wings. However, as large interference effects may occur when wings and bodies having low drag at transonic velocities are combined to form airplane-like configurations, tests of such configurations are necessary for a final evaluation of the effects of sweepback, fineness ratio, and other variations of airplane geometry.

The present paper reports the results of a test on one of a series of wing-body configurations. This series consists of a family of wings mounted on bodies of fineness ratio 12 identical with the bodies whose tests were reported in reference 2. For this test a 45° swept-back wing of constant chord was mounted at a position forward of the maximum diameter of the body. The results are presented as curves showing the variation of drag coefficient with Mach number for the complete configuration and each of its component parts. The drag coefficient for the body and wing are compared with results previously obtained by the free-fall method for an identical body without wings and for comparable straight and swept-back airfoils tested on cylindrical bodies.

APPARATUS AND METHOD

Test configuration.- The general arrangement of the configuration is shown in figure 1 and details and dimensions are given in figure 2. The 45° swept-back wing had a 70-inch span and incorporated an NACA 65-009 airfoil section of 12-inch chord perpendicular to the leading edge. The nominal aspect ratio of this wing (based on the wing area including that within the body) was 4.1. The wing was mounted on a 10-inch-diameter body of fineness ratio 12 externally identical with the bodies whose tests were reported in reference 2. The wing entered the body through rectangular slots and was attached to a force measuring balance in the body. A wooden

filler block faired to the body contour was attached to the wing root so that the clearance between the sides of the slot and the movable wing assembly was about 1/32 inch. The wing was located on the body so that the 50-percent-chord station at the wing root was approximately 15 inches forward of the body maximum diameter. The tail boom and fin arrangement were identical with the arrangement of reference 2. The tail fins passed through open slots 3/8 inch wide and 6 inches long in the tail boom and were attached to a force measuring balance.

Measurements.- Measurement of the desired quantities was accomplished as in previous tests (references 1 and 3) through use of the NACA telemetering system and radar and phototheodolite equipment. The following quantities were recorded at a ground station by the telemetering system:

(1) The force exerted by the wing on the body as measured by a spring balance

(2) The force exerted by the tail fins on the tail boom as measured by a spring balance

(3) The retardation of the configuration as measured by a sensitive accelerometer alined with the longitudinal axis by the body

(4) The total pressure at an orifice located at the nose of the body as measured by an aneroid cell

The flight path of the airplane from which the configuration was dropped was recorded up to the release point through use of the radar and phototheodolite equipment. A survey of atmospheric conditions at the time of the test was obtained from synchronized records of static pressure, temperature, and actual altitude during the descent of the airplane. The direction and velocity of the horizontal component of the wind in the altitude range of the test was determined from radar and phototheodolite records of the ascent of a free balloon just prior to the test.

Reduction of data.- At release, the velocity of the configuration with respect to the ground, hereafter referred to as the ground velocity, was obtained by differentiation of the flight path of the airplane up to the release point as recorded by the radar and phototheodolite equipment. The ground velocity of the configuration throughout the free fall was obtained by a step-by-step integration of the vector sums of the gravitational acceleration and the directed retardation as measured by the accelerometer.

Variation of altitude with time throughout the fall was determined by integration of the vertical components of the ground velocity. True airspeed was obtained by a vector summation of the ground velocity and the horizontal wind velocity at appropriate altitudes.

The total drag of the configuration was obtained directly by multiplying the retardation a_1 (in g units) by the weight of the configuration. The drag force on the wing D_W was determined through use of the relation

$$D_W = R_W + W_W a_1$$

where

R_W measured reaction between body and wing, pounds

W_W weight of movable wing assembly, pounds

The drag of the tail fins was obtained from the same relation by using the reaction between the fins and the tail boom and the weight of the movable fin assembly. Body drag was determined by subtracting the wing and tail drags from the total.

Values of drag D, static pressure p, absolute temperature T, and frontal area F were combined with the airspeed to obtain the Mach number M and the nondimensional parameter D/Fp for the complete configuration and each of its components. Values of the conventional drag coefficient based on frontal area C_{D_F} were obtained from simultaneous values of these parameters by use of the relation

$$C_{D_F} = \frac{D/Fp}{M^2\gamma/2}$$

where the ratio of specific heats γ was taken as 1.4. In the case of the wing and the tail fins, drag coefficients based on plan area C_D were obtained by multiplying C_{D_F} by the ratio of frontal area to plan area. The areas did not include that submerged in the body or tail boom.

RESULTS AND DISCUSSION

A time history of the important measured and computed quantities obtained from this test is given in figure 3. The altitude variation shown was computed from the accelerometer data. The total vertical

distance of the fall as obtained from these data agrees with the release altitude obtained from the radar and phototheodolite tracking records within 20 feet. Although the estimated accuracy of the telemetered accelerations was ±0.01 g units, this excellent agreement indicates that these accelerations and hence the total drag of the configuration were probably determined with better accuracy than estimated. In previous tests the ground velocity computed from the accelerometer data has been compared with the ground velocity computed from the flight path of the test body throughout the free fall as determined from radar and phototheodolite tracking records. Although these tracking records were not obtained for the present test, the previous tests have shown good agreement between the two methods for determining ground velocity. The two Mach number variations shown in figure 3 were determined from two independent sets of measurements. The solid curve was computed from the airspeed and temperature data and is believed to be accurate within ±0.01 in Mach number. The dashed curve of Mach number was computed from telemetered records of total pressure and the static pressure determined from the survey of the atmosphere. The estimated accuracy of the total-pressure measurements was ±2 percent of the full-scale value, which would give a corresponding Mach number error of ±0.05 at M = 1.0 and ±0.015 at M = 1.2. The data obtained, however, indicate that the accuracy of the total-pressure measurement was somewhat better than estimated.

The results of this test are presented in figures 4 to 7 as curves showing the variations of the parameter D/Fp and the drag coefficients for the complete configuration and its individual components. The drag forces were measured throughout the fall to within ±7 pounds for the complete configuration, $\pm 3\frac{1}{2}$ pounds for the wing, and $\pm 1\frac{1}{2}$ pounds for the tail. Since the static pressure increased during the drop, however, the accuracy with which the parameter D/Fp was determined also increased throughout the fall (or with increase in Mach number). At a given Mach number C_D and D/Fp have the same accuracy when these accuracy values are expressed as a fraction of the existing magnitude of C_D and D/Fp at that Mach number, except that the drag coefficients have a small additional uncertainty due to the possible error in Mach number (±0.01). The estimated accuracy for these drag parameters for several Mach numbers is presented in the following table:

Mach number	0.8			1.0			1.2		
Drag parameter	D/Fp	C_{D_F}	C_D	D/Fp	C_{D_F}	C_D	D/Fp	C_{D_F}	C_D
Total	0.011	0.028	------	0.007	0.017	------	0.003	0.007	------
Wing	.012	.029	0.0018	.009	.016	0.0010	.004	.008	0.0005
Tail	.032	.073	.0044	.023	.044	.0026	.010	.019	.0011
Body	.034	.078	------	.024	.037	------	.010	.013	------

The variations of D/Fp and drag coefficient based on total frontal area for the complete configuration are given in figure 4. The drag per unit frontal area rose from 0.06 of atmospheric pressure at a Mach number of 0.89 to 0.167 of atmospheric pressure at a Mach number of 1.02 and then increased at a slower rate at 0.233 at M = 1.19. When these data are transformed to drag coefficients the curve shows the usual abrupt rise starting at a Mach number of 0.89 which resulted in the drag coefficient increasing slightly more than two times at M = 1.02. The drag coefficient increased slightly over the remainder of the Mach number range. The cross hatching on figure 4 shows how the total drag of the configuration was divided among the components. At Mach numbers in excess of 1.0 the body and wing shared about equal portions of the total drag, or about 42 percent each. The remaining drag (about 16 percent) was that due to the tail.

The variations with Mach number of D/Fp and drag coefficients for the 45° swept-back wing as tested on this configuration are presented in figure 5. The drag per unit frontal area rose abruptly from 0.061 of atmospheric pressure at a Mach number of 0.95 to 0.147 atmospheric pressure at M = 1.0 and then increased more slowly to 0.257 at M = 1.19. The wing drag coefficients showed a small increase with Mach number in the region between M = 0.9 and M = 0.95 and then increased abruptly to a value at M = 1.0 slightly less than three times the value at M = 0.9. Further increase in Mach number resulted in a small increase in the wing drag coefficient to a value slightly greater than three times the low-speed value at the highest investigated velocity. The abrupt rise in drag for this swept-back wing, which occurred near the speed of sound, will be discussed later in this paper when the present results are compared with the results of previous tests of 45° swept-back airfoils by the same method.

Figure 6 shows the variations with Mach number of D/Fp and drag coefficients for the tail fins. The drag per unit frontal area

increased abruptly from 0.074 of atmospheric pressure at a Mach number of 0.9 to 0.385 atmospheric pressure at $M = 0.97$ and then increased almost linearly to 0.519 of atmospheric pressure at $M = 1.19$. The abrupt rise in drag coefficients for the tail fins peaked at $M = 0.97$ and then showed a slight decrease with further increase in Mach number. Similar data are presented in figure 6 for an identical tail arrangement which was mounted on the body of fineness ratio 6 without wings (reference 1). Generally the data of reference 1 and the present data are in good agreement, particularly as to the Mach number range over which the abrupt rise in drag took place and as to the magnitudes of drag in the highest portion of the investigated speed range. The discrepancies in the variations of the drag near $M = 1.0$ cannot result entirely from inaccuracies of measurement but are evidently caused to some extent by the differences in the flow field about the tail resulting from differences in the geometry of the two test configurations. It may be expected that the difference in the two tail drags would follow mainly from differences in the velocity and size of the wake behind the body, especially if the local static pressure in the vicinity of the tail fins has returned to the free-stream value.

The variations of the body drag parameters with Mach number as measured on this configuration, which are presented in figure 7, show an abrupt rise in drag beginning at a Mach number of 0.975. The drag per unit of frontal area increased to a value of 0.145 of atmospheric pressure at $M = 1.02$ and then increased more slowly to a value of 0.175 at $M = 1.19$. The drag coefficient based on body frontal area peaked at $M = 1.02$ and showed a slight decrease throughout the remainder of the investigated speed range. The cause of the irregular variation of drag with Mach number at Mach numbers in excess of 1 has not been definitely determined but possibly results from interference effects between wing and body. This condition is expected to be clarified in subsequent tests. An abrupt decrease in body drag is indicated between $M = 0.95$ and $M = 0.975$ where the abrupt drag rise occurred on the swept-back wing. It will be necessary to investigate this drag decrease further, however, since the percent error in the magnitude of the body drag parameters at Mach numbers less than unity may be rather large. Comparable data for the body whose test was reported in reference 2 are also presented in figure 7. This body was identical with the body of the present test and had the same tail fin arrangement; however, the body of reference 2 was tested without wings. Since data on the tail drag were not obtained for the tests of reference 2, the tail drags determined from the present tests were used to obtain the drag of the body previously tested. Because the drag rise on the tail occurs before the drag

rise on the body, the values of tail drag are of the same order as the body drag at Mach numbers slightly below the body drag rise. At these Mach numbers somewhat different tail drag variations due to differences in the flow field about the tail for the two tests could therefore have an appreciable effect on the body drag data as computed by subtracting the tail drag from the drag of the body-tail combination. For this reason, body drags computed from the data of reference 2 by this method are not presented in the range where the body drags are of the same order as the tail drags. Comparison of the body drags presented in figure 7 indicates that mounting the swept-back wing on the body had a detrimental effect on the body drag, for with this addition, the drag rise of the body took place at a slightly lower Mach number and higher drags appear to exist at Mach numbers above the drag rise (about 15 percent higher at $M = 1.05$ to 8 percent at $M = 1.15$).

Results of tests by the free-fall method of the present wing and a group of rectangular and 45° swept-back airfoils of constant chord which were mounted on cylindrical test bodies are summarized in figure 8. All of the airfoils for which data are presented had NACA 65-009 sections of constant chord perpendicular to the leading edge. The abrupt drag rise which occurred near the speed of sound for the present 45° swept-back wing did not occur for the other 45° swept-back airfoils previously tested. Prior to the drag rise, however, the drag obtained for the present wing was in good agreement with that obtained from the other tests. As a result of this drag rise the drag of the present wing was roughly double the value estimated from the previous results at $M = 1.0$ and 1.25 the value estimated at $M = 1.15$. The drag at Mach numbers in excess of unity was, however, only about 40 percent of the drag of comparable rectangular airfoils. All airfoil drag data presented in figure 8 for the previous tests were obtained from measurements on airfoils mounted near the rear of long cylindrical bodies, while the present wing was mounted forward of the maximum diameter of a body which tapered toward the front and the rear. The existence of an abrupt drag rise for the present swept-back wing which did not occur for the comparable swept-back wings previously tested indicates the transonic drag of swept-back wings may be critically dependent upon either the position of the wing on the body or the shape of the body at the wing-body juncture. In addition, the airfoils tested on cylindrical bodies entered the bodies through open rectangular slots and the unknown effect of these slots on the results obtained may alter the effect herein presented. Further investigation of the effect of such slots on the drag of swept-back wings will therefore be necessary.

CONCLUDING REMARKS

The drag of a wing-body configuration has been measured at transonic velocities by the free-fall method. This configuration consisted of a 45° swept-back wing mounted forward of the maximum diameter of a body of fineness ratio 12 which had been tested previously without wings.

The results show that the drag per unit frontal area of this configuration rose abruptly from 0.060 of atmospheric pressure at a Mach number of 0.89 to 0.167 of atmospheric pressure at a Mach number of 1.02 and then increased at a slower rate to 0.233 at a Mach number of 1.19. At Mach numbers in excess of unity the wing and body of the configuration shared about equal portions of the total drag (about 42 percent each). The remaining drag was contributed by the stabilizing tail surfaces.

Near the speed of sound the drag of the tested wing rose abruptly to double the value estimated from previous tests of 45° swept-back airfoils which were mounted on cylindrical bodies. After this abrupt rise the drag approached the values estimated from the previous tests. This condition would indicate that in the transonic region the drag of swept-back wings is critically dependent upon the position of the wing on the body and/or the shape of the body, particularly at the wing-body juncture. The body drags obtained from this test were higher than those measured in previous tests of an identical body without wings by about 15 percent at a Mach number of 1.05 and 8 percent at 1.15. These results show that unfavorable interference effects exist for the tested wing-body configuration; the drag of the swept-back wing was considerably increased in the presence of the body and the drag

of the body appeared to be somewhat increased in the presence of the wing.

Langley Memorial Aeronautical Laboratory
National Advisory Committee for Aeronautics
Langley Field, Va.

REFERENCES

1. Bailey, F. J., Jr., Mathews, Charles W., and Thompson, Jim Rogers: Drag Measurements at Transonic Speeds on a Freely Falling Body. NACA ACR No. L5E03, 1945.

2. Thompson, Jim Rogers, and Mathews, Charles W.: Total Drag of a Body of Fineness Ratio 12 and Its Stabilizing Tail Surfaces Measured during Free Fall at Transonic Speeds. NACA CB No. L6D08, 1946.

3. Mathews, Charles W., and Thompson, Jim Rogers: Drag Measurements at Transonic Speeds of NACA 65-009 Airfoils Mounted on a Freely Falling Body to Determine the Effects of Sweepback and Aspect Ratio. NACA RM No. L6K08c, 1947.

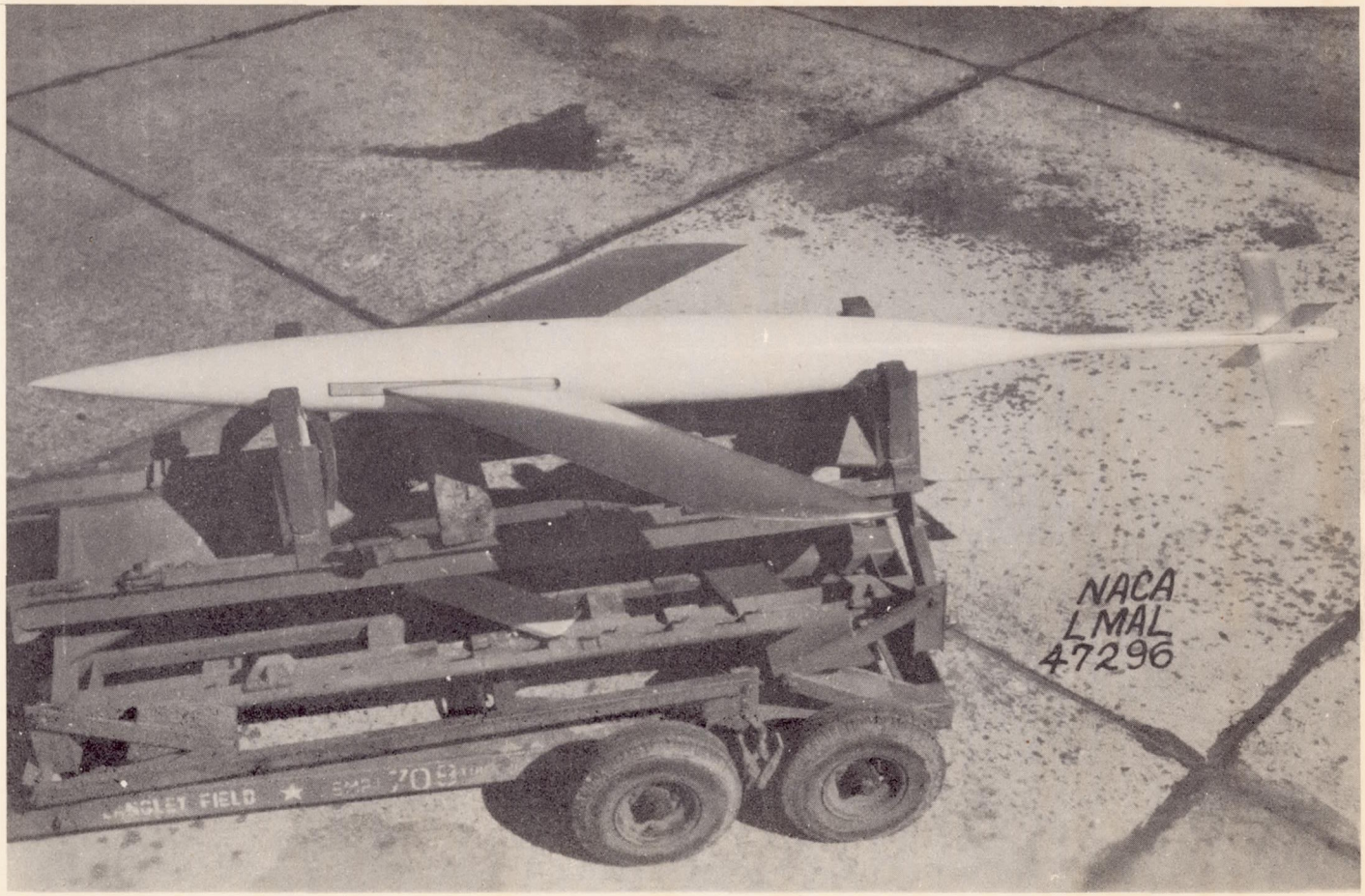

Figure 1.- General view of wing-body configuration.

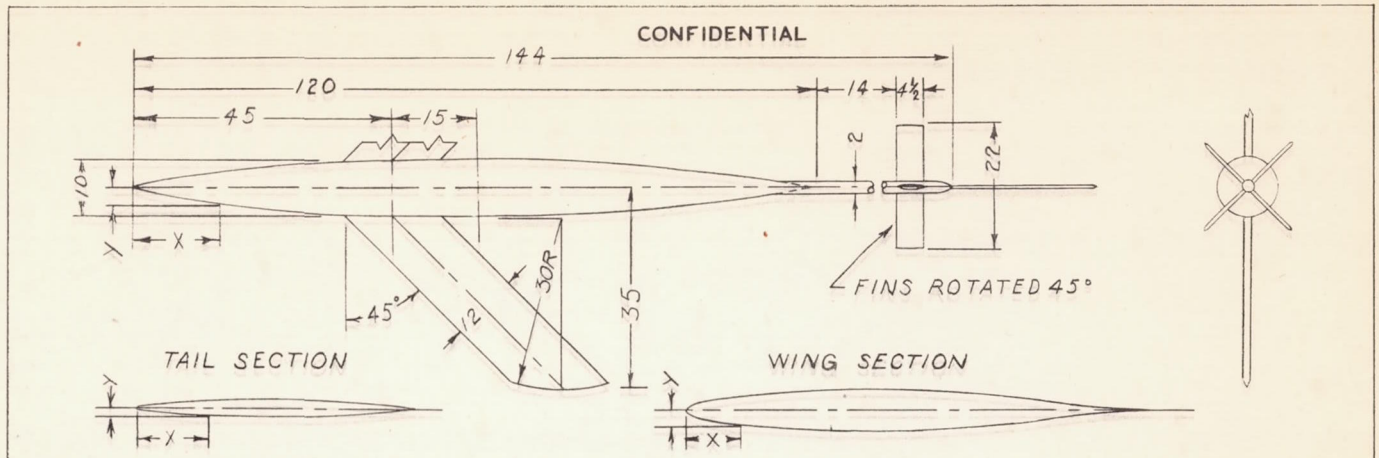

DIMENSIONS SQ.FT.

BODY FRONTAL AREA	0.545	WING PLAN AREA	6.990
WING FRONTAL AREA	.438	TAIL PLAN AREA	1.232
TAIL FRONTAL AREA	.074	TOTAL FRONTAL AREA	1.057

WING-SECTION COORDINATES (NACA 65-009 SECTION)

X	Y	X	Y	X	Y
0.000	0.000	2.400	.447	7.800	.398
.060	.083	3.000	.486	8.400	.342
.090	.102	3.600	.512	9.000	.280
.150	.127	4.200	.531	9.600	.216
.300	.171	4.800	.540	10.200	.151
.600	.235	5.400	.537	10.800	.088
.900	.286	6.000	.520	11.400	.033
1.200	.328	6.600	.490	12.000	.000
1.800	.396	7.200	.448		

L.E. RADIUS 0.066

TAIL-SECTION COORDINATES (NACA 16-SECTION AIRFOIL)

X	Y	X	Y
0.000	0.000	1.350	.122
.052	.029	1.800	.132
.113	.041	2.250	.135
.225	.056	2.700	.131
.338	.068	3.150	.118
.450	.078	3.600	.094
.675	.093	4.050	.057
.900	.105	4.275	.032
1.125	.115	4.500	.003

L.E. RADIUS 0.008

BODY COORDINATES

X	Y	X	Y
0.000	0.000	48.000	4.876
.600	.277	54.000	4.971
.900	.358	60.000	5.000
1.500	.514	66.000	4.955
3.000	.866	72.000	4.828
6.000	1.446	78.000	4.610
9.000	1.936	84.000	4.274
12.000	2.365	90.000	3.754
18.000	3.112	96.000	3.031
24.000	3.708	102.000	3.222
30.000	4.158	108.000	2.350
36.000	4.489	114.000	.526
42.000	4.719	120.000	.000

NOSE RADIUS 0.060

CONFIDENTIAL

NATIONAL ADVISORY COMMITTEE FOR AERONAUTICS

Figure 2.- General arrangement and dimensions of wing-body configuration. All dimensions are in inches. Wing sections measured perpendicular to leading edge.

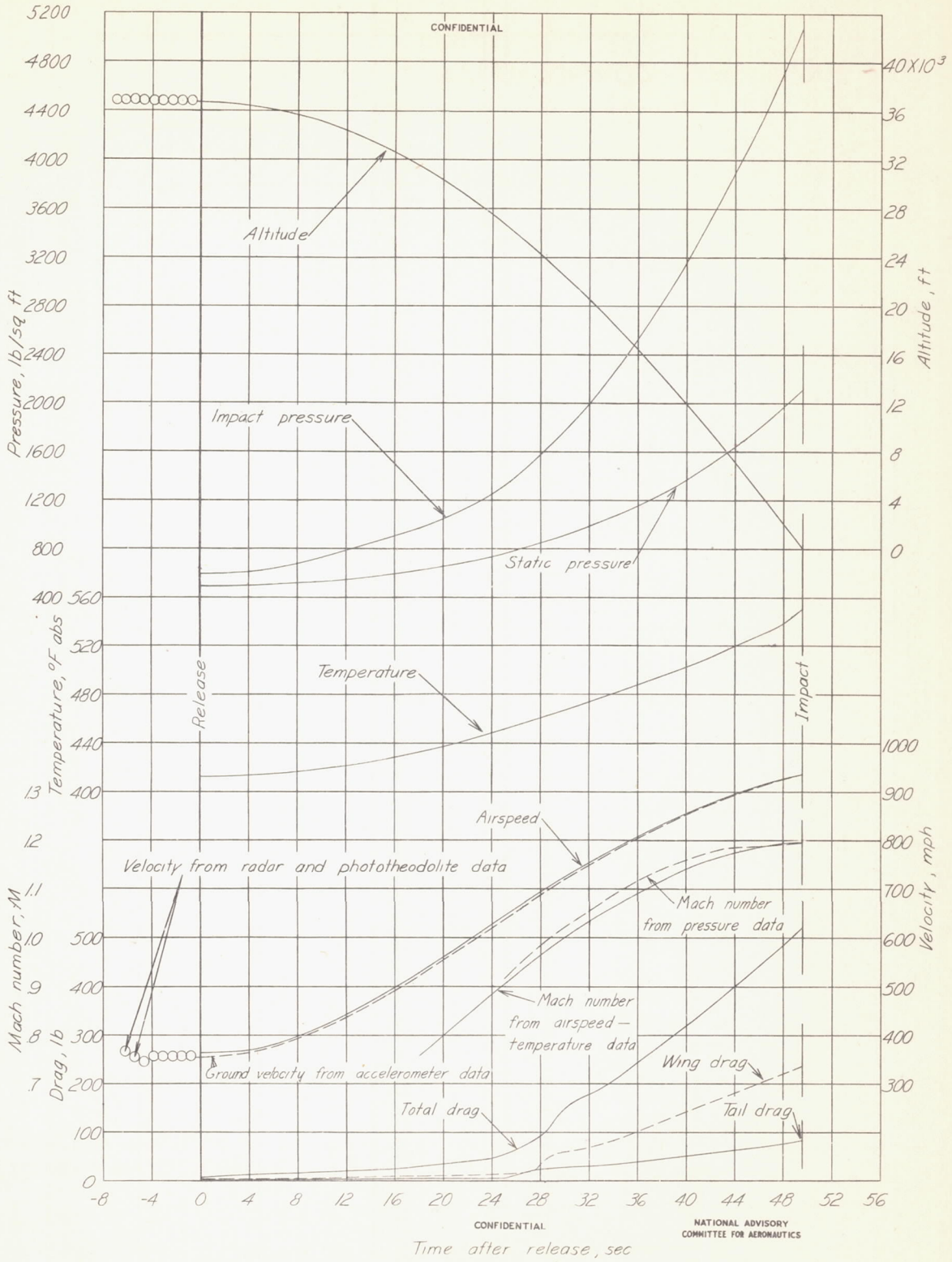

Figure 3.- Time history of free fall of wing-body configuration.

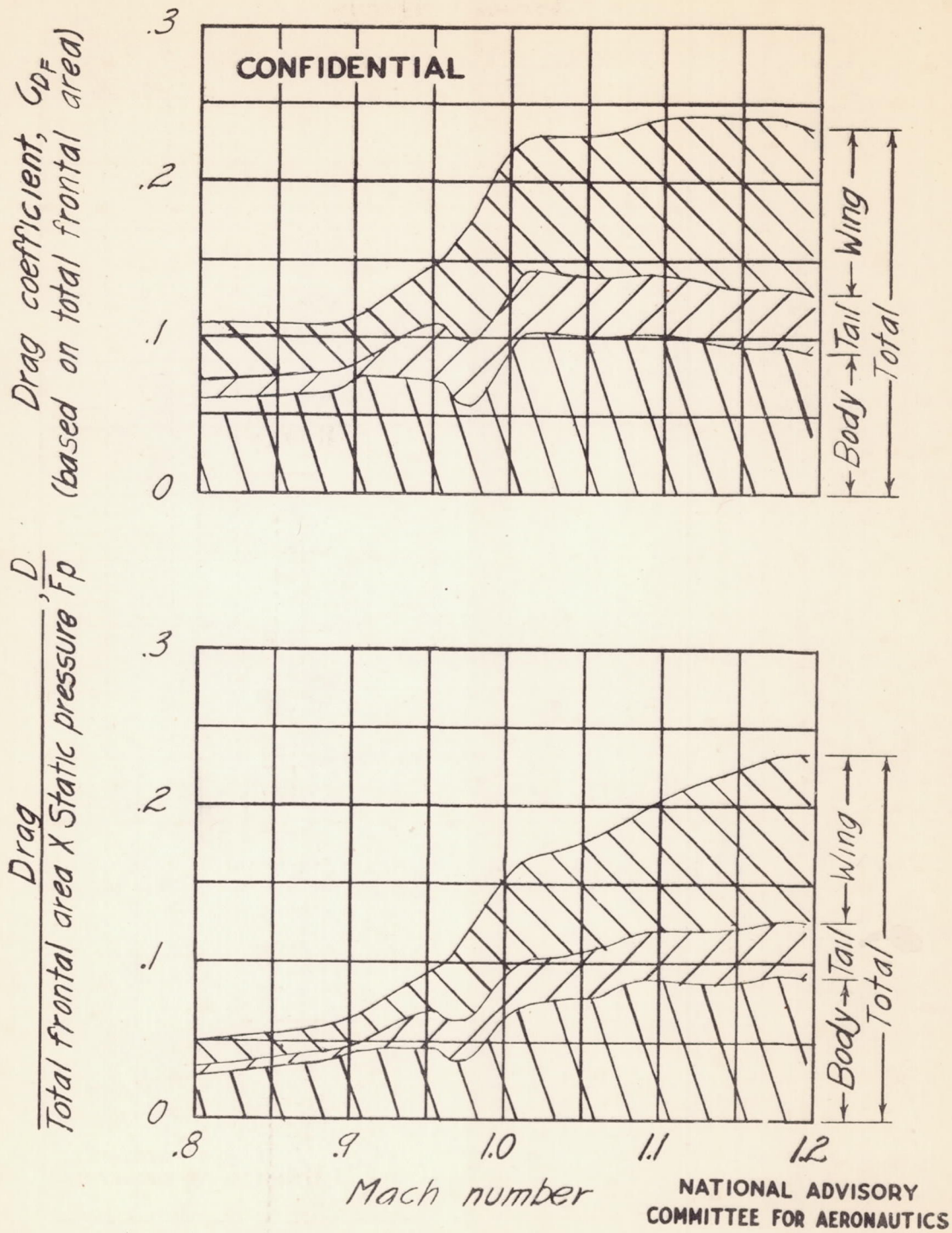

Figure 4.- Variation with Mach number of drag coefficient and D/F_p for the complete configuration.

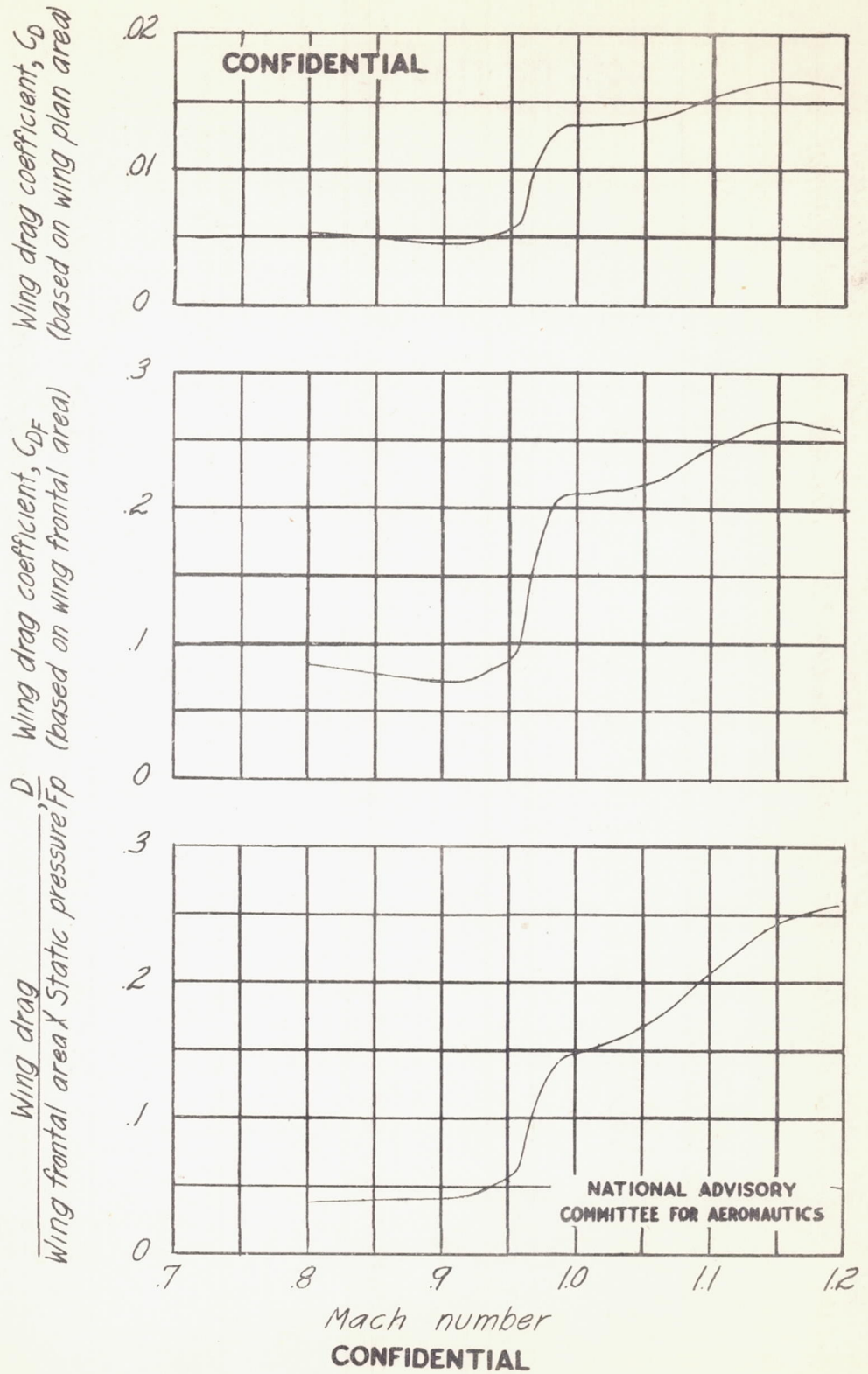

Figure 5.- Variation with Mach number of drag coefficients and D/F_p for the 45° swept-back wing of the tested configuration.

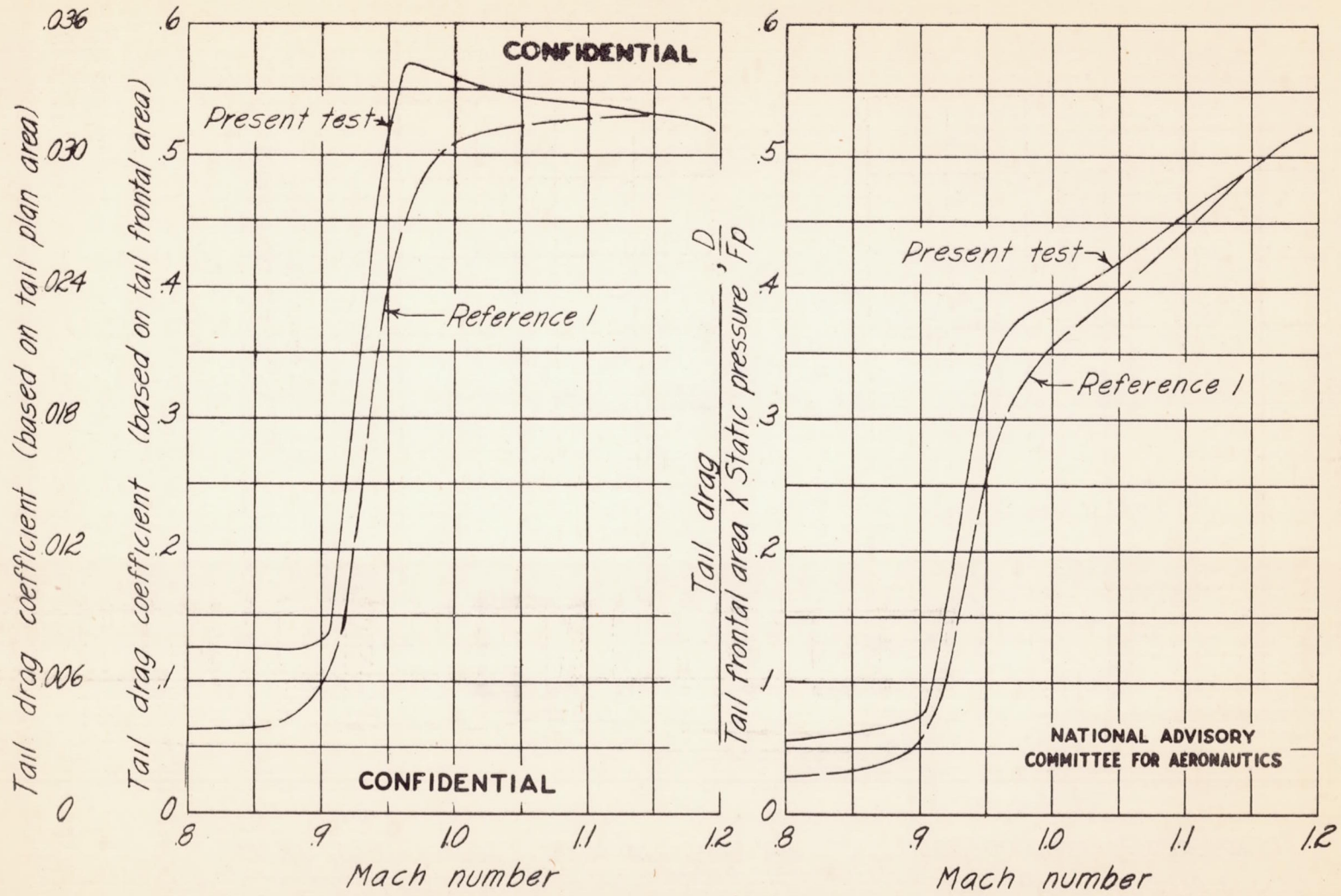

Figure 6.- Variation with Mach number of drag coefficients and D/F_p for the tail fins of the tested configuration. Data for identical tail fins mounted on a body of fineness ratio 6 taken from reference 1.

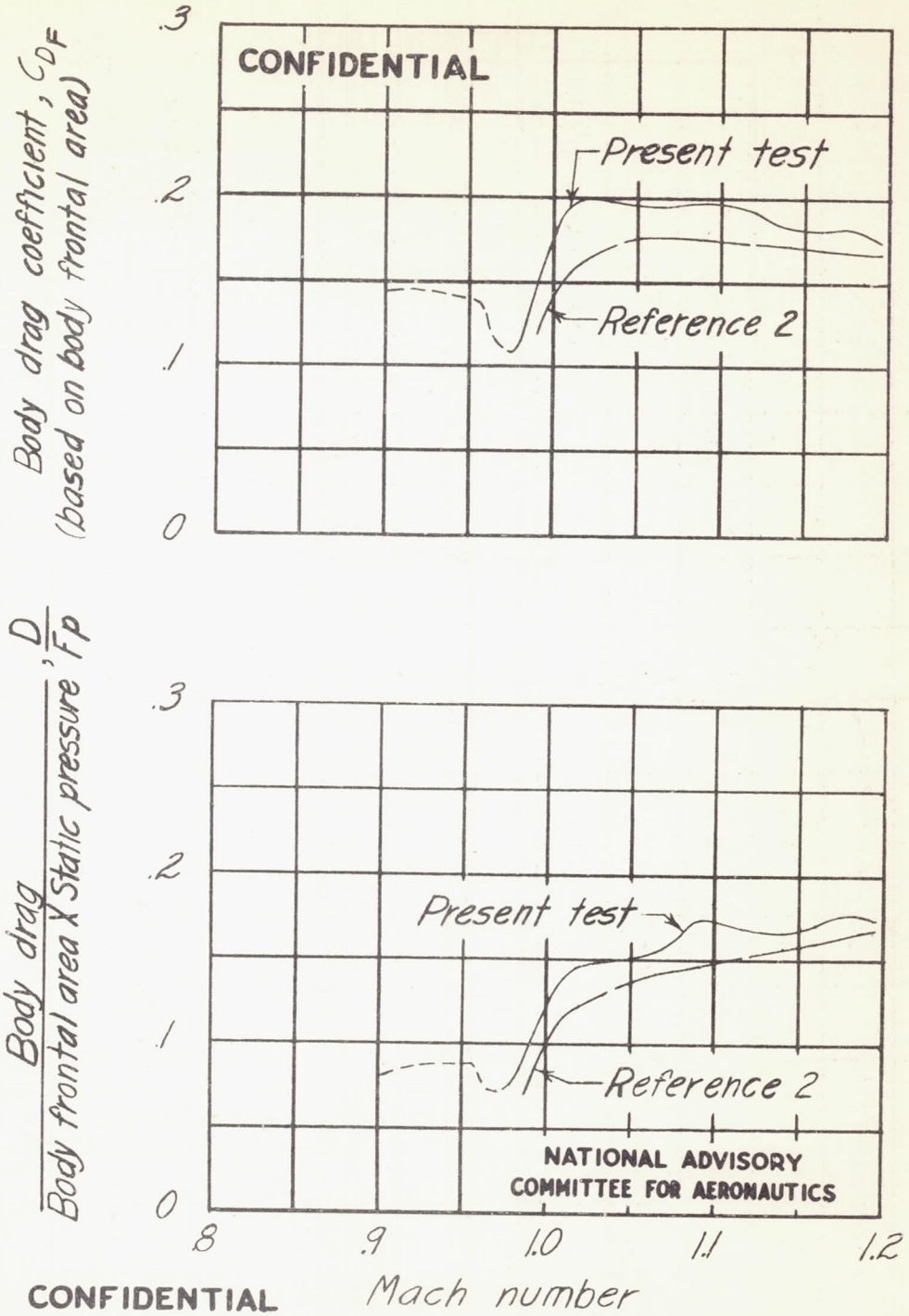

Figure 7.- Variation with Mach number of drag coefficient and D/F_p for the body of the tested configuration. Data for identical body without wings taken from reference 2.

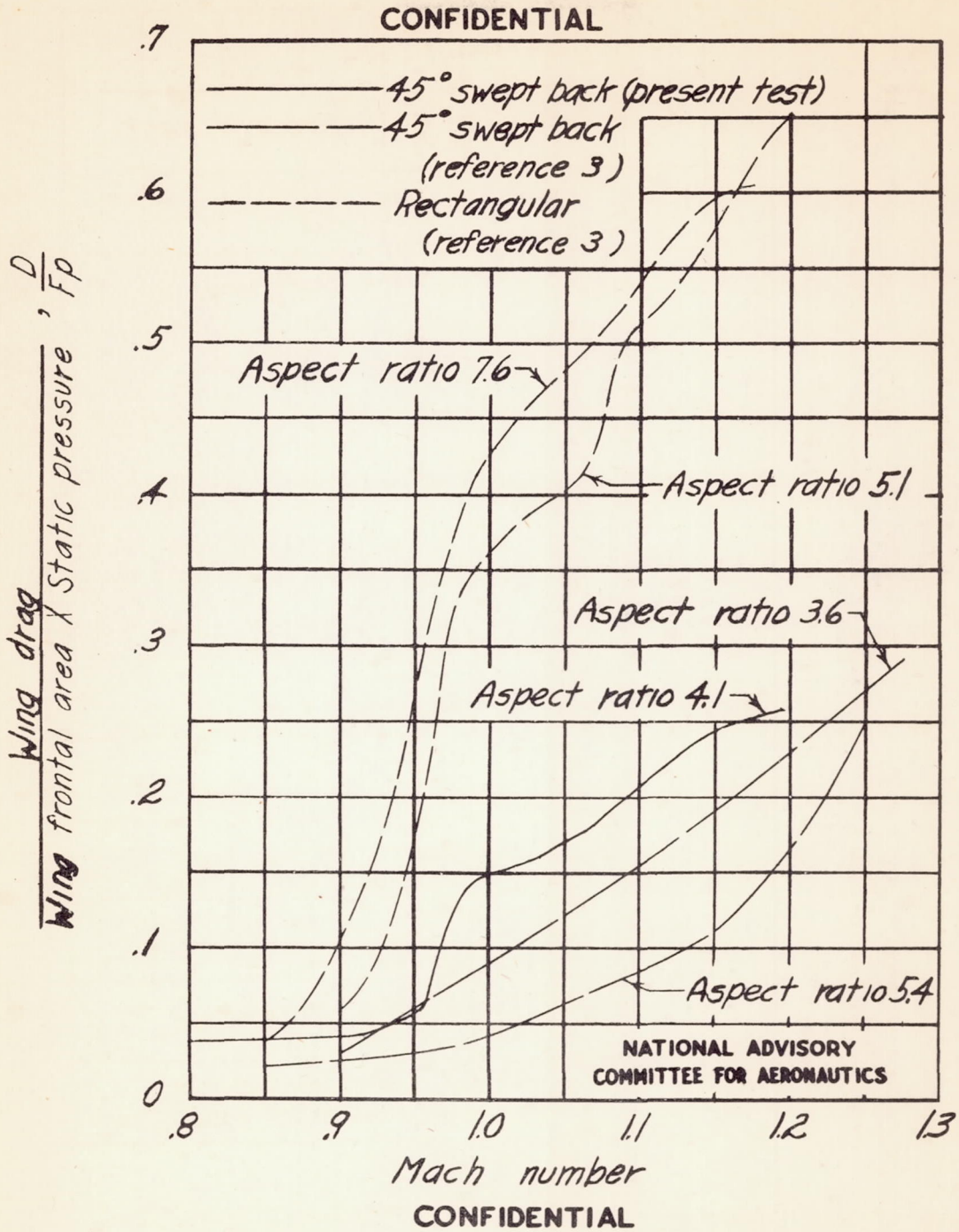

Figure 8.- Comparison curves showing variation with Mach number of D/F_p for the present wing and comparable rectangular and swept-back airfoils mounted on cylindrical bodies. Airfoil data taken from reference 3.